Theoretical Investigation of the Reaction between Aluminum and Propene. Comparison between Calculated and Experimental ESR Results

Torbjörn Fängström,*,† Leif A. Eriksson,‡ and Sten Lunell†

Department of Quantum Chemistry, Uppsala University, Box 518, S-751 20 Uppsala, Sweden, and Department of Physics, Stockholm University, Box 6730, S-113 85 Stockholm, Sweden

Received: February 13, 1997; In Final Form: April 22, 1997[⊗]

Stationary points on the potential energy surface describing the reaction between aluminum and propene have been optimized at the MP2 and DFT (B3LYP, BLYP, BP86, and PWP86) levels using the 6-31G(d,p) basis set, including ZPE and BSSE corrections. All methods are found to give very similar geometrical structures and MP2, MP4, and DFT potential energy surfaces, although some variations exist. An initial addition complex is formed between Al and C_3H_6, located 6−15 kcal/mol below the free reactants in energy. Passing over a transition state barrier of 15−25 kcal/mol, an asymmetric cyclic *trans*-π-allylaluminum hydride product is formed at energies similar to the addition complex. A small barrier separates this product from the energetically most stable conformer, *cis*-π-allylaluminum hydride. Hyperfine coupling constants (hfcc's) of Al and the protons were computed at all stable structures, using MP2 and DFT methods and the 6-311G-(d,p), 6-311+G(2df,p), and IGLO-III (PWP86 only) bases. The hfcc calculations clearly confirm the *cis*-π-allylaluminum hydride as being the structure observed experimentally.

I. Introduction

Several experimental investigations of reactions between aluminum atoms and small organic molecules such as ethylene,[1−3] acetylene,[2,4] buta-1,3-diene,[5] propyne,[6] benzene,[7] and several ethers[8−10] have been presented during the last 25 years. Also a number of theoretical works on the abovementioned reactions and/or its products have been performed, cf. refs 11−16. Recently, Histed et al. reported on the reaction of ground-state aluminum atoms with propene on inert hydrocarbon surfaces at 77 K using electron spin resonance (ESR) techniques.[17] They observed a superimposed ESR spectrum from three paramagnetic species. One of the spectra was assigned to allyl and a second to dimethyl-substituted aluminocyclopentane. The main interest was focused on the third species, whose ESR spectrum shows hyperfine structures with isotropic splittings of a 336 G sextet, a 57.4 G doublet, a 13.5 G triplet, and a 5.2 G doublet. This suggested two equivalent hydrogens (the triplet) and two unique hydrogens (the two doublets). It was also noted that the doublet splitting of 57.4 G was similar to that of the unique hydrogen of methylaluminum hydride CH_3AlH.[17,18] Products obtained in reactions using selectively deuterated propenes and aluminum atoms demonstrated that the hydrogen attached to the aluminum atom was transferred from a methyl group and that the two equivalent hydrogens are not bound to the same carbon nucleus.[17] On the basis of the abovementioned observations, Histed et al. considered this product to be a cyclic π-allylaluminum hydrid.

In the present work we have performed a detailed theoretical study of the reaction of atomic Al with propene. Stationary points on the potential energy surface (PES) have been located and hyperfine coupling constants (hfcc's) are calculated for the different products. A variety of basis sets and theoretical approaches have been employed, ranging from semiempirical to correlated perturbation theory and the more novel density functional theory (DFT) levels of theory.

II. Methods

A. Geometries. To find first guesses to possible transition states and energy minima on the potential energy surface, the semiempirical PM3[19,20] method as implemented in the Spartan program package[21] was used. Five different addition complexes, nine products, and seven transition states were located. Starting from the PM3 geometries, full geometry optimizations were then performed at the correlated ab initio or density functional theory levels, leading to a significantly reduced number of stationary points. In all these calculations the program systems Gaussian-92[22] and Gaussian-94[23] were used. Electron correlation was included through Møller−Plesset perturbation theory[24] to second order (MP2). For all geometry optimizations and energy calculations at the MP2 level, the frozen core approximation was employed. Three different functionals were used in the DFT calculations, referred to as B3LYP, BLYP, and BP86, respectively. The B3LYP functional is based on Becke's three-parameter adiabatic connection method (ACM) approach and consists of a combination of Slater,[25] Hartree−Fock,[26] and Becke[27] exchange and the Vosko, Wilk, and Nusair (VWN) local[28] and Lee, Yang, and Parr (LYP)[29] nonlocal correlation functional. The BLYP functional is built from the nonlocal exchange functional by Becke,[27] the VWN local correlation functional, and the nonlocal LYP correlation functional. The BP86 functional, finally, has the same exchange part as in BLYP, together with Perdew's gradient corrected correlation functional.[30] The split valence 6-31G(d,p)[31,32] basis set was used in all ab initio and DFT optimizations. The product structures were finally also optimized using a fourth functional (PWP86[33−35]) and the larger IGLO-III[36] basis set as implemented in the deMon[37−40] program.

B. Energies. To obtain more reliable values of the energies for the different stationary points on the PES, a number of single-point calculations using larger basis sets or other methods were performed. This will also enable us to evaluate the overall performance of the lower levels of theory. For the stationary points on the MP2/6-31(d,p) potential surface, MP4(SDTQ)/6-31G(d,p)[41] as well as MP2 calculations with the larger 6-311+G-(2df,p) basis set[42−46] were performed. Similarly, for all

† Department of Quantum Chemistry.
‡ Department of Physics.
[⊗] Abstract published in *Advance ACS Abstracts,* June 1, 1997.

S1089-5639(97)00552-5 CCC: $14.00

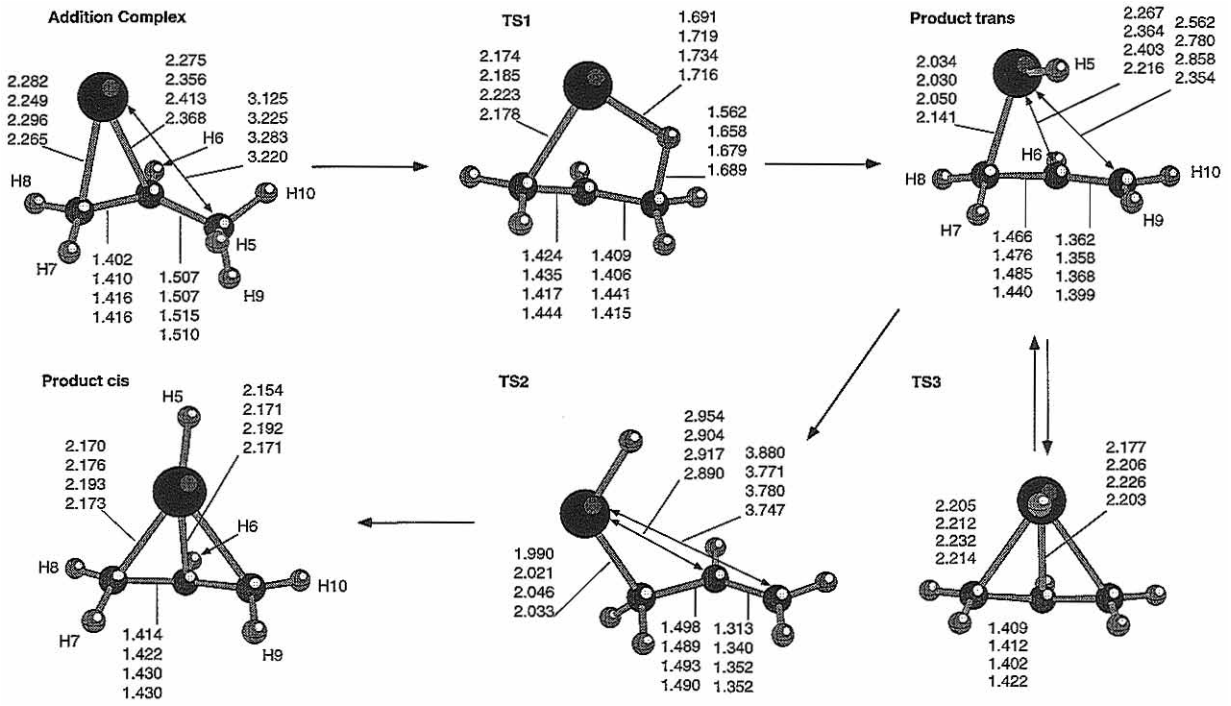

Figure 1. Addition complex transition states and products at MP2/6-31G(d,p), B3LYP/6-31G(d,p), BLYP/6-31G(d,p), and BP86/6-31G(d,p) levels. Some carbon−carbon and Al−carbon distances, in Å, are indicated. The distances are ordered starting from the top, as obtained in the calculations using the MP2, B3LYP, BLYP, and BP86 methods. The suggested reaction path is indicated by arrows.

stationary points on the DFT/6-31G(d,p) potential surfaces, single-point calculations were carried out at the same DFT level using the 6-311+G(2df,p) basis.

To specify a certain level of approximation used in a geometry optimization the notation "method/basis" is used throughout the present paper, *e.g.*, BP86/6-31G(d,p) implies a geometry optimization employing the BP86 functional and the 6-31G-(d,p)basis. In a similar fashion, to specify the level employed for a single point calculation at a geometry optimized at different level of approximation the notation "method A/basis a//method B/basis b" is used *e.g.*, BP86/6-311+G(2df,p)//MP2/6-31G(d,p) implies a single-point calculation employing the BP86 functional and the 6-311+G(2df,p) basis at a geometry optimized employing Møller−Plesset perturbation theory to second order in conjunction with the 6-31G(d,p) basis.

C. Isotropic Hyperfine Coupling Constants. Hyperfine splittings arise from interactions between the nuclear spin ($\vec{I}$) and the electronic magnetic moments, caused by the electron spin ($\vec{S}$) and angular momentum. The splittings can be divided into an isotropic and an anisotropic part, where the isotropic part is given by a contact interaction (Fermi contact) term[47,48] in the spin Hamiltonian:

$$H^{(1)}_{\text{spin}} = A_{\text{N}}^{(\text{iso})}(\vec{I}\cdot\vec{S}) \qquad (1)$$

For a particular nucleus N (assuming a doublet radical), $A_{\text{N}}^{(\text{iso})}$ is

$$A_{\text{N}}^{(\text{iso})} = (8\pi/3)g\beta g_{\text{N}}\beta_{\text{N}}\rho^{(\alpha-\beta)}(\vec{r}_{\text{N}}) \qquad (2)$$

Where $\rho^{(\alpha-\beta)}(\vec{r}_{\text{N}})$ is the spin density at the position of the particular nucleus N. The isotropic hfcc's are thus related to the spin density at a particular nucleus, which can be obtained from a calculated wave function. Hence, comparison with measured hyperfine splittings gives a good indication of the quality of the calculated wave function and the ability of the method in question to accurately describe the system under study. We here report hfcc's for the Al atom and for the hydrogens for those points on the potential energy surface believed to be possible reaction products. Results are presented from the MP2, B3LYP, BLYP, and BP86 calculations using the 6-311G(d,p) and 6-311+G(2df,p) bases and from the PWP86 calculations using the IGLO-III basis.

III. Results

A. Geometry Optimizations. *1. MP2 Level.* Of the five PM3-optimized addition complexes (AC), only one could be found at the MP2/6-31G(d,p) level (Figure 1). In the addition complex the Al atom is mainly interacting with the double bond in the propene molecule, causing an elongated C═C distance. Out of nine PM3-optimized product structures, in which one of the methyl group protons has migrated to Al, only three survived at the MP2/6-31(d,p) level of theory. These are one cyclic *cis*-like structure and two cyclic *trans* structures (cf. Figure 1). The cyclic *cis* structure has almost C_s symmetry with the mirror plane cutting through the Al, the mid carbon, H_5, and H_6 atoms. The deviation from a completely symmetric structure is not more than 0.01 Å for the C−C bond length and 0.02 Å for the Al−C bond length. Also one of the *trans* structures is close to a C_s symmetric structure, with no larger deviations than 0.001 Å in the C−C bond distances and 0.004 Å in the Al−C bond distances at this level of approximation. The deviations from symmetric structures could be related to the very shallow shape of the PES.

Two different transition states were furthermore located at this level of theory, one which connects the addition complex with the asymmetric cyclic *trans* conformer (TS1) and one which connects this *trans* structure to the cyclic *cis* form (TS2). In TS1, hydrogen H_5 has migrated toward the Al atom and the structure corresponds to a five-membered ring (see Figure 1). In TS2, the Al atom binds only to one carbon forming an open chain structure in which the migrated hydrogen is occupying a position half-way between its position in the *cis* and *trans* products.

To verify the products to be true minima, frequency calculations were performed at the stationary points. At the MP2/6-

31G(d,p) level the frequencies for the cyclic *cis* structure and for the asymmetric cyclic *trans* structure were all real, whereas the symmetric cyclic trans structure exposed one imaginary frequency and can accordingly not be considered as a true minima. The symmetric cyclic *trans* structure is most likely a transition state (TS3) connecting the asymmetric cyclic trans structure and its mirror image. Finally, frequency calculations verified TS1 and TS2 to be saddle points of first order.

2. The Density Functional Approach. Similar investigations of the possible addition complexes, transition states, and products were performed using the three functionals B3LYP, BLYP, and BP86 together with the 6-31G(d,p) basis set. All DFT functionals were found to yield very similar results as the MP2 level of theory. Also here only one addition complex was obtained for each functional, starting from structures resembling those found at the PM3 level of approximation. The DFT-optimized addition complexes are all rather similar to the complex found at the MP2 level, with the one difference that the distances between the mid carbon and the aluminum atom are somewhat longer compared to the MP2/6-31G(d,p) result. Hence, at the DFT levels, the aluminum atom binds more clearly to only one of the terminal α-carbon atoms. The product structures found at the DFT levels were again very similar to those at the MP2 level (one cyclic *cis* structure and two cyclic *trans* structures, one symmetric and one asymmetric). Just as for the MP2 level the *cis* structure and one of the *trans* structures are close to being of C_s symmetry with no larger deviations from a completely symmetric structure than at most 0.015 Å in the C−C bond distances and 0.03 Å in the Al−C bond distances. Two transition states highly similar to the ones found at MP2/6-31G(d,p) level were also found for the three functionals. One transition state (TS1) is connecting the addition complex and the asymmetric cyclic *trans* structure, and the other transition state (TS2) connects the asymmetric *trans* structure with the symmetric *cis* structure as for the MP2 level. Frequency calculations were performed and again the symmetric *trans* structures exposed one small imaginary frequency using the B3LYP and BLYP functionals.

Using the BP86 functional, a slightly asymmetric transition state, resembling the symmetric *trans* structure, was obtained which was verified to be a transition state structure in a frequency calculation. The symmetric *trans* structure, on the other hand, exposed no imaginary frequency. Hence on the BP86/6-31G(d,p) surface the symmetric *trans* structure corresponds to a energy minimum with a slightly asymmetric transition state connecting to the asymmetric *trans* structure. The potential energy surface in the vicinity of the symmetric *trans* structure at the BP86 level is very flat, the energy difference between the symmetric *trans* structure and the slightly asymmetric transition state is not more than 0.02 kcal/mol. Also, the smallest frequency for the symmetric *trans* structure is only 47 cm^{-1} and the imaginary frequency for the slightly asymmetric transition structure is 35i cm^{-1}.

Both at the MP2 level and at the DFT levels, six points of interest have thus been located on the potential energy surface: One addition complex, three transition states (TS1, TS2, and TS3), one *trans* product, and one *cis* product. The structures found at the different levels of theory are very similar in shape, the one exception being the addition complex, in which a somewhat larger difference in geometry is seen between the MP2 and BLYP levels of theory (cf. Figure 1). The largest differences are in the two longest Al−C distances, which are 0.14 and 0.16 Å shorter, respectively, at the MP2 level. In TS1 the main difference is the distance between the C atom and the migrating hydrogen, the C−H distance being 0.13 Å shorter at

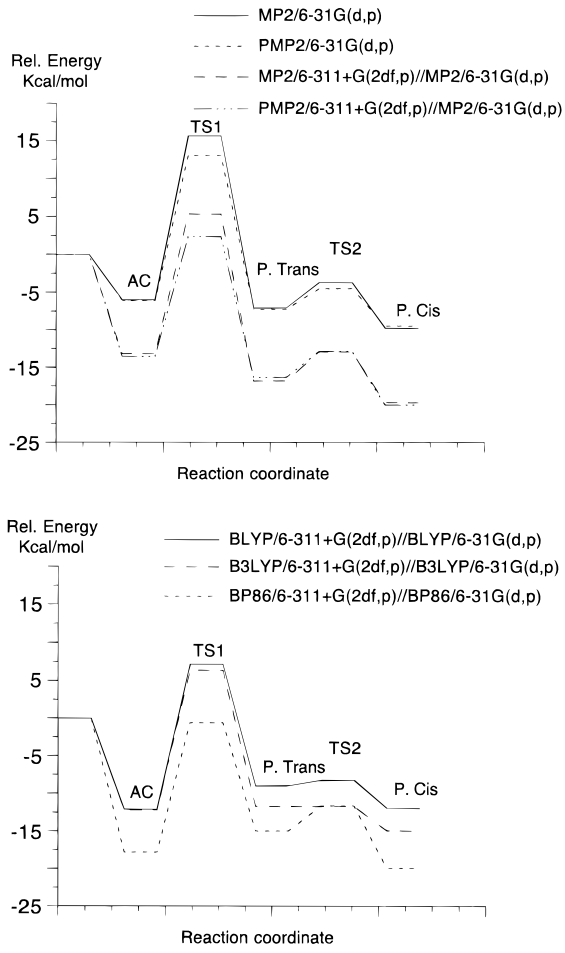

Figure 2. (a) Relative energy as a function of the reaction coordinate at the (P)MP2/6-31G(d,p) and (P)MP2/6-311+G(2df,p)//MP2/6-31G(d,p) levels of theory. BSSE corrections are calculated and included at the (P)MP2/6-31G(d,p) and (P)MP2/6-311+G(2df,p)//MP2/6-31G(d,p) levels. ZPE corrections, calculated at the B3LYP/6-31G(d,p) level, are also included in all energy profiles, see text. (b) Relative energy as a function of the reaction coordinate at DFT/6-311+G(2df,p)//DFT/6-31G(d,p) levels of theory. BSSE corrections are calculated and included at the B3LYP/6-311+G(2df,p)//B3LYP/6-31G(d,p) level. ZPE corrections, calculated at the B3LYP/6-31G(d,p) level, are also included at this level of approximation.

the MP2 level compared with the BP86 results. Another somewhat larger difference in geometry is found for the *trans* product, in which the largest Al−C distance differs 0.5 Å between the BP86 and BLYP functionals. For the same distance the difference is 0.3 Å between the MP2 and BLYP structures.

To verify the relevance of the transition states found, intrinsic reaction coordinate IRC[49,50] calculations were performed starting from the transition states. Due to the close similarity in geometric structures between the different methods, intrinsic reaction coordiate (IRC) calculations were performed only at the B3LYP/6-31G(d,p) level. The points connected via TS1 were confirmed to be the addition complex and the asymmetric cyclic *trans* structure, and the points connected via TS2 were the asymmetric cyclic *trans* structure and the symmetric cyclic *cis* structure. Finally, an IRC calculation was performed at the B3LYP/6-31G(d,p) level starting from TS3 (cyclic symmetric *trans* structure). As suggested earlier, this was confirmed as a TS connecting the cyclic asymmetric *trans* structure to its mirror image.

B. Potential Energy Surfaces. *1. MP2 and MP4 Surfaces.* The relative energies of the MP2/6-31G(d,p) optimized stationary points are presented in Table 1 and Figure 2a. The energy of the addition complex is 11.2 (11.6) kcal/mol below the

TABLE 1: Relative Energies for Various Levels of Approximations in kcal/mol for Stationary Points at MP2/6-31(d,p) Level of Theory

	structure						
method	react	AC	TS1	*trans* product	TS2	*cis* product	TS3
MP2/6-31G(d,p)	−359.390 17	−11.19	12.01	−10.84	−4.95	−13.80	−10.29
PMP2/6-31G(d,p)//MP2/6-31G(d,p)	−359.390 94	−11.65	9.07	−10.84	−5.64	−14.61	−10.20
MP2/6-31G(d,p) + BSSE	−359.390 17	−5.59	18.65	−4.60	−0.30	−7.14	
PMP2/6-31G(d,p)//MP2/6-31G(d,p) + BSSE	−359.390 94	−5.70	16.07	−4.77	−1.11	−7.15	
MP2/6-31G(d,p) + BSSE + ZPE[a]	−359.390 17	−6.00	15.61	−7.07	−3.71	−9.75	
PMP2/6-31G(d,p)//MP2/6-31G(d,p) + BSSE + ZPE[a]	−359.390 94	−6.11	13.03	−7.24	−4.53	−9.46	
MP3/6-31G(d,p)//MP2/6-31G(d,p)	−359.433 05	−9.10	18.13	−5.40	−1.28	−8.60	−4.04
PMP3/6-31G(d,p)//MP2/6-31G(d,p)	−359.433 40	−9.49	15.96	−5.52	−1.91	−8.38	−4.08
MP4/6-31G(d,p)//MP2/6-31G(d,p)	−359.455 98	−9.60	14.93	−6.19	−1.26	−8.94	−5.28
PMP4/6-31G(d,p)//MP2/6-31G(d,p)	−359.456 34	−9.99	12.76	−6.32	−1.88	−9.59	−5.32
MP2/6-311+G(2df,p)//MP2/6-31G(d,p)	−359.512 56	−14.84	5.86	−16.80	−11.37	−19.84	−16.56
PMP2/6-311+G(2df,p)//MP2/6-31G(d,p)	−359.514 02	−15.24	2.83	−16.34	−11.29	−20.19	−16.04
MP2/6-311+G(2df,p)//MP2/6-31G(d,p) + BSSE	−359.512 56	−12.81	8.35	−14.34	−9.55	−17.08	
PMP2/6-311+G(2df,p)//MP2/6-31G(d,p) + BSSE	−359.514 02	−13.14	5.40	−13.87	−9.47	−17.39	
MP2/6-311+G(2df,p)//MP2/6-31G(d,p) + BSSE + ZPE[a]	−359.512 56	−13.23	5.31	−16.81	−12.97	−19.69	
PMP2/6-311+G(2df,p)//MP2/6-31G(d,p) + BSSE + ZPE[a]	−359.514 02	−13.55	2.36	−16.34	−12.89	−20.00	

[a] The ZPE corrections are calculated at B3LYP/6-31G(d,p) level (see text).

energies of the reactants at the MP2 (PMP2) level. The transition state connecting the asymmetric cyclic *trans* conformer to the addition complex, TS1 is 12.0 kcal/mol above the energies of the reactants at the MP2 level and 9.1 kcal/mol above at the PMP2 level. This gives a barrier for the Al insertion of 23.2 kcal/mol at the MP2 level and 20.7 kcal/mol at the PMP2 level using the smaller 6-31G(d,p) basis. The energy of the most stable product, the *cis* conformer, is 13.8 kcal/mol below the reactants at the MP2 level and 14.6 kcal/mol at the PMP2 level, i.e., 3−4 kcal/mol lower in energy than the cyclic *trans* product. The transition state connecting the asymmetric cyclic *trans* conformer and the cyclic *cis* conformer, TS2, lies some 5−6 kcal/mol above the asymmetric *trans* structure, and TS3, which is connecting the *trans* product with its mirror image, lies 0.6 kcal/mol above the *trans* product at the MP2/6-31G(d,p) and PMP2/6-31G(d,p) levels of theory.

Only small differences between the MP2 and PMP2 energies are seen for all stationary points except for the transition state. This close similarity between the MP2 and PMP2 levels is also seen in the small deviation of $\langle S^2 \rangle$ from the ideal value of 0.75. $\langle S^2 \rangle$ is at most 0.78 except for the transition state for which a somewhat larger value of 0.84 is found.

To check the effects of basis set superposition errors (BSSEs), the counterpoise correction[51] method was applied to TS1 and to the addition complex. Also for TS2 and the product structures the BSSEs were calculated, this time using Al−H and allyl as reactants. In all those calculations at the MP2 level, the frozen core approximation was again employed.

Zero-point vibrational energy corrections (ZPE) were calculated for all stationary points. This was done only at the B3LYP/6-31G(d,p) level, the motivation for this being, on one hand, the close similarity of the MP2 and DFT geometries at the stationary points (cf. Figure 1) and, on the other hand, earlier findings showing that ZPE calculated at the B3LYP/6-31G(d,p) level often are as good as or better than the ones calculated at the MP2/6-31G(d,p) level.[52]

The effect of the counterpoise correction and zero-point vibrational energy corrections (ZPE calculated at the B3LYP/6-31G(d,p) level) at the MP2/6-31G(d,p) and PMP2/6-31G(d,p) levels of approximation for all stationary points, except TS3, is shown in Table 1. The inclusion of the corrections causes a minor energy increase of 1.1−5.5 kcal/mol for all points. The counterpoise correction increases the energy for all points by 4.5−7.5 kcal/mol. The ZPE on the other hand stabilizes the product structures 0.4−3.4 kcal/mol (using the B3LYP ZPE). Correcting for the BSSE and ZPE, the Al insertion barrier decreases from 23.2 to 21.6 kcal/mol at the MP2/6-31G(d,p) level and from 20.7 to 19.1 kcal/mol at the PMP2/6-31G(d,p) level. The overall energy profile for the reaction is not changed more than about 3 kcal/mol when the corrections are included (cf. Table 1).

At the (P)MP4/6-31G(d,p)//MP2/6-31(d,p) level (Table 1), the two product structures increase in energy relative to the reactants by 4.5−5 kcal/mol, with the most stable product, the cyclic *cis* conformer, now lying 9.6 kcal/mol below the reactants at the PMP4/6-31G(d,p)//MP2/6-31(d,p) level. The addition complex increases by about 1.5−2 kcal/mol and the transition states TS1 and TS2 ca. 3−4 kcal/mol at those levels of theory. Thus the barrier to Al insertion increases by a few kilocalories per mole compared to the (P)MP2/6-31G(d,p) level without corrections. Also listed in Table 1 are the MP3 energies, which are in between the MP2 and MP4 values, though in general closer to the MP4 values. If instead of increasing the level of theory (MP2 to MP4), we increase the basis set from 6-31G(d,p) to 6-311+G(2df,p) at the MP2 (PMP2) level, an overall stabilization of all stationary points on the surface is observed (also Figure 2a). The relative energies for the products decrease about 5−6 kcal/mol compared to the MP2/6-31G(d,p) level. Similarly, the addition complex drops in energy by 3.5−4 kcal/mol and the transition state TS1 by about 6 kcal/mol. The Al insertion energy barrier is now of 20.7 kcal/mol at the MP2/6-311+G(2df,p)//MP2/6-31(d,p) level and 18.1 kcal/mol at the PMP2/6-311+G(2df,p)//MP2/6-31(d,p) level. Also at this level, BSSE corrections were calculated for all stationary points except TS3, the corrections due to the ZPE were taken from the B3LYP/6-31G(d,p) level, see discussion above. The corrections destabilized the addition complex and the product structures by up to 1.7 kcal/mol and stabilized the transition state conformers 0.5−1.6 kcal/mol. The Al insertion energy barrier, including the corrections, drops a few kilocalories per mole compared to the uncorrected values to 18.5 kcal/mol, MP2/6-311+G(2df,p)//MP2/6-31(d,p), and to 15.9 kcal/mol, PMP2/6-311+G(2df,p)//MP2/6-31(d,p), (cf. Figure 2a).

2. DFT Surfaces. In Table 2 and in Figure 2b, finally, we list the energies of the DFT/6-31G(d,p) optimized structures as well as those obtained from single-point calculations using the larger 6-311+G(2df,p) basis. As mentioned earlier, the geometries found for the stationary points in the DFT calculations are all rather similar to the geometries obtained at the MP2 level of theory. With BP86 the entire curve is shifted some 6−10

TABLE 2: Relative Energies in kcal/mol for Stationary Points at DFT/6-31(d,p) Level

	structure						
method	react	AC	TS1	*trans* product	TS2	*cis* product	TS3
B3LYP/6-31G(d,p)	−360.284 85	−12.67	9.19	−8.90	−6.38	−12.15	−7.85
B3LYP/6-31G(d,p) + BSSE	−360.284 85	−11.08	11.00	−6.69	−4.66	−9.84	
B3LYP/6-31G(d,p) + ZPE	−360.284 85	−13.08	6.15	−11.37	−9.8	−14.76	
B3LYP/6-31G(d,p) + BSSE + ZPE	−360.284 85	−11.49	7.96	−9.16	−8.08	−12.45	
BLYP/6-31G(d,p)	−360.192 08	−12.77	6.83	−8.52	−6.40	−11.99	−7.39
BP86/6-31G(d,p)	−360.269 78	−17.81	−0.29	−14.60	−9.67	−19.23	−14.65
B3LYP/6-311+G(2df,p)//B3LYP/6-31G(d,p)	−360.337 10	−12.27	8.90	−9.84	−8.74	−12.94	−8.34
B3LYP/6-311+G(2df,p)//B3LYP/6-31G(d,p) + BSSE	−360.337 10	−11.81	9.40	−9.26	−8.31	−12.35	
B3LYP/6-311+G(2df,p)//B3LYP/6-31G(d,p) + ZPE[a]	−360.337 10	−12.68	5.86	−12.31	−12.16	−15.55	
B3LYP/6-311+G(2df,p)//B3LYP/6-31G(d,p) + BSSE + ZPE[a]	−360.337 10	−12.22	6.36	−11.73	−11.73	−14.96	
BLYP/6-311+G(2df,p)//BLYP/6-31G(d,p)	−360.249 40	−12.11	7.15	−9.04	−8.26	−11.99	−7.36
BP86/6-311+G(2df,p)//BP86/6-31G(d,p)	−360.321 79	−17.82	−0.60	−14.99	−11.65	−19.96	−14.91
PWP/IGLO-III	−360.6064 11			−20.22		−24.94	−19.91

[a] The ZPE corrections are calculated at B3LYP/6-31G(d,p) level (see text).

TABLE 3: Experimental and Theoretical Hyperfine Coupling Constants for Products Obtained at MP2/6-31G(d,p) Level[a]

	structure						
method	Al	H_5	H_6	H_7	H_8	H_9	H_{10}
				cis Product			
MP2/6-311G(d,p)//MP2/6-31G(d,p)	358.0	49.8	−2.1	9.2	−1.5	9.2	−1.5
B3LYP/6-311G(d,p)//MP2/6-31G(d,p)	350.7	63.7	−4.6	12.7	0.8	12.7	0.9
BLYP/6-311G(d,p)//MP2/6-31G(d,p)	340.5	64.5	−4.5	13.0	0.8	13.0	0.8
BP86/6-311G(d,p)//MP2/6-31G(d,p)	331.1	54.1	−4.6	12.3	0.8	12.4	0.8
exptl	336	57.4	5.2	13.5		13.5	
				trans Product			
MP2/6-311G(d,p)//MP2/6-31G(d,p)	332.1	55.5	9.9	−3.0	−1.5	−10.3	−9.7
B3LYP/6-311G(d,p)//MP2/6-31G(d,p)	330.2	69.7	1.6	2.2	−0.3	0.1	0.7
BLYP/6-311G(d,p)//MP2/6-31G(d,p)	323.5	69.1	1.7	2.6	−0.3	0.2	0.7
BP86/6-311G(d,p)//MP2/6-31G(d,p)	316.9	58.3	1.5	2.4	−0.1	0.2	0.8
exptl	336	57.4	5.2			13.5	13.5

[a] The hfcc are reported from calculations using the MP2 and DFT approaches together with the 6-311G(d,p) basis.

kcal/mol toward increased relative stability of the stationary points, compared with the other methods. The insertion barrier is lowest at the BP86 level, 17.5 kcal/mol, and highest at the B3LYP level, 21.9 kcal/mol.

When counterpoise corrections are included at the B3LYP/6-31G(d,p) level, an increase in energy is seen for all structures of about 1.5−2.3 kcal/mol. Including the ZPE causes a small, 0.4 kcal/mol, stabilization for the addition complex and a larger, 2.5−3.5 kcal/mol, stabilization for the transition states and products. Altogether the counterpoise correction and ZPE causes a small stabilization in energy for the transition states and products of at most 1.7 kcal/mol and a destabilization of 1.2 kcal/mol for the addition complex at the B3LYP/6-31G-(d,p) level.

The deviations of $\langle S^2 \rangle$ from the ideal value of 0.75 are even smaller for the DFT methods than for the MP2 method. The maximum value of $\langle S^2 \rangle$ among all functionals tested here is 0.76.

The effects of increasing the basis set from 6-31G(d,p) to 6-311+G(2df,p) are small (within 2.5 kcal/mol) for all DFT functionals tested. This should be compared with the (P)MP2 results, where an increased basis led to a considerably larger (5−6 kcal/mol) lowering of the energies of the stationary points. Inclusion of the BSSE corrections estimated at the B3LYP/6-311+G(2df,p)//B3LYP/6-31G(d,p) level of theory and the ZPE calculated at B3LYP/6-31G(d,p) level gave an increase in energy of less than 0.1 kcal/mol for the addition complex and an decrease in energy between 1.9 and 3.0 kcal/mol for TS1, TS2, and the products. The inclusion of the corrections at this level of approximation almost makes the small energy barrier between the *trans* and *cis* product disappear (cf Table 2 and Figure 2b). Calculations for the two products and TS3 at the PWP/IGLO-III level of theory produced the energetically most stable results, the *cis* product being 25 kcal/mol below the reactants in energy and with the *trans* product 4.7 kcal/mol and TS3 5 kcal/mol less stable compared to the *cis* product (cf. Table 2).

IV. Hyperfine Coupling Constants

A. MP2 Geometries. The hfcc's were calculated for the hydrogens and the aluminum atoms of the addition complex and products at both the MP2 level and the DFT levels using all three functionals. In the single-point calculations using the MP2 method all molecular orbitals, including the core, were used in the correlation treatment. Two basis sets were used in calculations for the hfcc's, one smaller (6-311G(d,p)) and one larger (6-311+G(2df,p)). The best overall agreement between experimental and calculated values is observed for the *cis* structure, also supported by the calculated energetic stability of the products. Using the MP2/6-31G(d,p) geometry for the cyclic *cis* structure, almost all methods and basis sets give a reasonable agreement between calculated and experimental hfcc's, cf Tables 3 and 4. All methods except BP86 gives somewhat too large hfcc values for the Al atom; a value that decreases by a few gauss with all methods when the basis is increased. For the hydrogens, increasing the basis set has little or no effect on the hfcc's. The values of A_{iso}(Al) obtained from the BLYP calculations are in excellent agreement with experiment. For the hydrogen H_5, attached to Al, the two functionals B3LYP and BLYP give slightly too large values, irrespective of the basis set used, but are still in good agreement with experiment. The rest of the methods underestimate the value of this same hfcc; the BP86 functional performed the best. All other proton hfcc's, irrespective of method and basis set, are too small relative to the experimental values. Best overall agreement between experimental and calculated values is observed for the BP86 functional and the smaller basis. The

TABLE 4: Experimental and Theoretical Hyperfine Coupling constants for Products Obtained at MP2/6-31G(d,p) Level[a]

	structure						
method	Al	H_5	H_6	H_7	H_8	H_9	H_{10}
				cis Product			
MP2/6-311+G(2df,p)//MP2/6-31G(d,p)	356.9	50.9	−2.0	9.1	−1.8	9.2	−1.7
B3LYP/6-311+G(2df,p)//MP2/6-31G(d,p)	348.3	64.1	−4.4	12.7	0.8	12.7	0.8
BLYP/6-311+G(2df,p)//MP2/6-31G(d,p)	337.8	64.9	−4.3	12.9	0.7	13.0	0.7
BP86/6-311+G(2df,p)//MP2/6-31G(d,p)	328.6	54.3	−4.5	12.2	0.6	12.2	0.6
exptl	336	57.4	5.2	13.5		13.5	
				trans Product			
MP2/6-311+G(df,p)//MP2/6-31G(d,p)	333.5	55.9	9.1	−2.9	−1.4	−9.3	−8.7
B3LYP/6-311+G(2df,p)//MP2/6-31G(d,p)	329.0	70.3	1.7	1.9	−0.3	0.1	0.7
BLYP/6-311+G(2df,p)//MP2/6-31G(d,p)	322.0	70.0	1.8	2.2	−0.3	0.1	0.7
BP86/6-311+G(2df,p)//MP2/6-31G(d,p)	315.6	58.9	1.5	2.1	−0.2	0.2	0.7
exptl	336	57.4	5.2			13.5	13.5
				Addition Complex			
B3LYP/6-311+G(2df,p)//MP2/6-31G(d,p)	10.4	5.0	1.1	−0.7	0.4	22.1	3.6
BLYP/6-311+G(2df,p)//MP2/6-31G(d,p)	7.8	5.0	1.7	−0.2	0.9	22.3	3.5
BP86/6-311+G(2df,p)//MP2/6-31G(d,p)	6.1	4.8	1.1	−0.8	0.3	21.3	3.3

[a] The hfcc are reported from calculations using the MP2 and DFT approaches together with the 6-311+G(2df,p) basis.

TABLE 5: Experimental and Theoretical Hyperfine Coupling constants for Products Obtained at MP2/6-31G(d,p) and DFT/6-31G(d,p) Levels[a]

	structure						
method	Al	H_5	H_6	H_7	H_8	H_9	H_{10}
				cis Product			
MP2/6-311+G(2df,p)//MP2/6-31G(d,p)	356.9	50.9	−2.0	9.1	−1.8	9.2	−1.7
B3LYP/6-311+G(2df,p)//B3LYP/6-31G(d,p)	345.5	64.9	−4.7	13.6	0.8	13.7	0.9
BLYP/6-311+G(2df,p)//BLYP/6-31G(d,p)	335.5	66.6	−4.7	13.9	0.8	14.1	0.9
BP86/6-311+G(2df,p)//BP86/6-31G(d,p)	321.3	54.2	−5.0	13.5	0.7	13.6	0.7
PWP/IGLO-III	345.4	60.1	−5.4	14.8	1.0	14.8	1.0
exptl	336	57.4	5.2	13.5		13.5	
				trans Product			
MP2/6-311+G(df,p)//MP2/6-31G(d,p)	333.5	55.9	9.1	−2.9	−1.4	−9.3	−8.7
B3LYP/6-311+G(2df,p)//B3LYP/6-31G(d,p)	305.7	71.2	1.5	3.1	−1.0	0.2	0.4
BLYP/6-311+G(2df,p)//BLYP/6-31G(d,p)	292.4	71.7	1.5	3.6	−1.3	0.2	0.3
BP86/6-311+G(2df,p)//BP86/6-31G(d,p)	360.6	68.5	0.9	−0.3	0.8	0.0	1.3
PWP/IGLO-III	317.9	70.1	−1.2	1.3	3.9	0.3	3.9
exptl	336	57.4	5.2			13.5	13.5
				Addition Complex			
B3LYP/6-311+G(2df,p)//B3LYP/6-31G(d,p)	10.6	5.4	−2.4	2.1	4.0	24.6	4.8
BLYP/6-311+G(2df,p)//BLYP/6-31G(d,p)	7.2	4.2	−1.9	1.5	3.7	23.4	5.3
BP86/6-311+G(2df,p)//BP86/6-31G(d,p)	5.8	4.5	−2.0	1.3	2.6	23.3	4.8

[a] The hfcc are reported from calculations using the MP2 and DFT approaches together with the 6-311+G(2df,p) basis.

assignment of the experimentally observed proton and Al hfcc is at this level as follows: Al, exptl value 336 G, calcd 331 G; H_5, exptl value 57.4 G, calcd 54.1 G; H_6, exptl value 5.2 G, calcd 4.6 G; H_7 and H_9, exptl value 13.5 and 13.5 G, calcd 12.3 and 12.4 G (cf. Figure 1 and Table 3). Calculated hfcc's are also reported for the addition complex and *trans* product (cf. Tables 3−5).

B. DFT Geometries. Only minor changes in the calculated hfcc's occur when the DFT-optimized geometries are used. In comparison with experimental data, the value assigned to the Al atom worsens slightly for the BP86 functional, while the values assigned to the hydrogens improve somewhat at this level. The changes for the two remaining functionals are all less than 3 gauss (cf. Tables 4 and 5). Also, values reported from the PWP86/IGLO-III calculations for the *cis* structure are in good agreement with the experimental values, although not as good as for those of the BP86 functional (cf. Table 5).

V. Summary and Discussion

Stationary points have been located for the reaction between aluminum and propene at the MP2, B3LYP, BLYP, and BP86 levels. All methods gives qualitatively the same result although the barriers and, especially, the absolute energies differ depending on method. The BP86/6-311+G(2df,p)//BP86/6-31G(d,p) and the BSSE and ZPE corrected PMP2/6-311+G(2df,p)//MP2/6-31G(d,p) methods give the lowest insertion barriers, 17.2 and 15.9 kcal/mol, respectively, and the BP86 and PWP86 functionals give the lowest relative energies for the products. All the methods tested here give very similar geometric structures.

A possible reaction path for the Al + propene insertion reaction is suggested. On the basis of the results in this theoretical investigation, the Al atom breaks a C−H bond of the methyl group to eventually form a cyclic (H)Al−allyl complex. The reaction path involves an Al−C_α addition complex, a transition state leading to a cyclic *trans* structure in which one hydrogen has migrated to the Al atom, whereafter the most stable structure on the potential surface, a cyclic *cis* structure, is reached through a second transition state.

The hyperfine coupling constants for the possible products have been determined using different basis sets in conjunction with the MP2 and DFT methods. There is good agreement between the computed and experimental hfcc's for only one of the products found, the cyclic *cis* structure. This supports the suggested reaction path toward a cyclic (H)Al−allyl complex

as the final product in the reaction. Best overall agreement between calculated and experimental hfcc's is obtained at the BP86/6-311+G(2df,p)//BP86/6-31G(d,p) level of theory, in which the calculated values differ at most 6% from the experimental (cf. Table 5). Due to the close similarity between the MP2 and DFT geometries, only minor changes are, however, seen in the calculated hfcc when using the geometry obtained with the MP2 method instead of the BP86 functional. The hfcc's obtained with all the DFT functionals lie within 17% of the experimental ones irrespective of the method used to determine the geometry. At the MP2 level the deviation between experimental and calculated hfcc varies; the larger couplings (Al and H_5) lie within 13% of the experimental while the smaller (H_6, H_7, and H_9) deviate by as much as 30−60%.

Acknowledgment. This work was supported by the Swedish National Science Research Council (NFR). A grant of computer time on the Cray C90 of the Swedish Supercomputer Center (NSC) in Linköping is gratefully acknowledged.

References and Notes

(1) Kasai, P. H.; McLeod, P., Jr. *J. Am. Chem. Soc.* **1975**, 97, 5609.
(2) Kasai, P. H. *J. Am. Chem. Soc.* **1982**, 104, 1165.
(3) Howard, J. A.; Mile, B.; Tse, J. S.; Morris, H. *J. Chem. Soc., Faraday Trans.* **1987**, *83*, 3701.
(4) Kasai, P. H.; McLeod, P., Jr.; Watanabe, T. *J. Am. Chem. Soc.* **1977**, *99*, 3521.
(5) Chenier, J. H. B.; Howard, J. A.; Tse, J. S.; Mile, B. *J. Am. Chem. Soc.* **1985**, *107*, 7290.
(6) Skell, P. S.; Wolf, L. R. *J. Am. Chem. Soc.* **1972**, *94*, 7919.
(7) Kasai, P. H.; McLeod, P., Jr. *J. Am. Chem. Soc.* **1979**, *101*, 5860.
(8) Parnis, J. M.; Mitchell, S. A.; Rayner, D. M.; Hackett, P. A. *J. Phys. Chem.* **1988**, *92*, 3869.
(9) Howard, J. A.; Joly, H. A.; Mile, B. *J. Chem. Soc., Faraday Trans.* **1990**, *86*, 219.
(10) Chenier, J. H.; Howard, J. A.; Joly, H. A.; LeDuc, M.; Mile, B. *J. Chem. Soc., Faraday Trans.* **1990**, *86*, 3321.
(11) Sakai, S. *J. Phys. Chem.* **1993**, *97*, 8917.
(12) Silva, S. J.; Head, J. D. *J. Am. Chem. Soc.* **1992**, *114*, 6479.
(13) Cramer, C. J. *J. Mol. Struct. (THEOCHEM)* **1991**, *235*, 243.
(14) Trenary, M.; Casida, M. E.; Brooks, B. R.; Schaefer, H. F., III *J. Am. Chem. Soc.* **1979**, *101*, 1638.
(15) Jing, S. Q.; Xie, Y.; Schaefer, H. F., III *Chem. Phys. Lett.* **1990**, *170*, 301.
(16) Fox, D. J.; Ray, D.; Rubesin, P. C.; Schaefer, H. F., III *J. Chem. Phys.* **1980**, *73*, 3246.
(17) Histed, M.; Howard, J. A.; Morris, H.; Mile, B. *J. Am. Chem. Soc.* **1988**, *110*, 5290.
(18) Parnis, J. M.; Ozin, G. A. *J. Am. Chem. Soc.* **1986**, *108*, 1699.
(19) Stewart, J. J. P. *J. Comput. Chem.* **1989**, *10*, 209.
(20) Stewart, J. J. P. *J. Comput. Chem.* **1989**, *10*, 221.
(21) *Spartan*, Version 4.0: Wavefunction, Inc.: 18401 Von Karman Ave., 370 Irvine, CA, 92715, 1995.
(22) Frisch, M. J.; Trucks, G. W.; Schlegel, H. B.; Gill, P. M. W.; Johnson, B. G.; Wong, M. W.; Foresman, J. B.; Robb, M. A.; Head-Gordon, M.; Repogle, E. S.; Gomperts, R.; Andres, J. L.; Raghavachari, K.; Binkley, J. S.; Gonzalez, C.; Martin, R. L.; Fox, D. J.; Defrees, D. J.; Baker, J.; Stewart, J. P.; Pople, J. A. *Gaussian 92/DFT*, Revision G.3, Gaussian, Inc.: Pittsburgh, PA, 1993.
(23) Frisch, M. J.; Trucks, G. W.; Schlegel, H. B.; Gill, P. M. W.; Johnson, B. G.; Robb, M. A.; Cheeseman, J. R.; Keith, T.; Petersson, G. A.; Montgomery, J. A.; Raghavachari, K.; Al-Laham, M. A.; Zakrzewski, V. G.; Ortiz, J. V.; Foresman, J. B.; Cioslowski, J.; Stefanov, B. B.; Nanayakkara, A.; Challacombe, M.; Peng, C. Y.; Ayala, P. Y.; Chen, W.; Wong, M. W.; Andres, J. L.; Repogle, E. S.; Gomperts, R.; Martin, R. L.; Fox, D. J.; Binkley, J. S.; Defrees, D. J.; Baker, J.; Stewart, J. P. Head-Gordon, M.; Gonzalez, C.; Pople, J. A. *Gaussian 94*, Revision B.2; Gaussian, Inc.: Pittsburgh, PA, 1995.
(24) Møller, C.; Plesset, M. S. *Phys. Rev.* **1934**, *46*, 618.
(25) Slater, J. C. *Quantum Theory of Molecular and Solids*; McGraw-Hill: New York, 1974, Vol. 4 (The Self-Consistent Field for Molecular and Solids).
(26) Fock, V. *Z. Phys.* **1930**, *61*, 126.
(27) Becke, A. D. *Phys. Rev. A* **1988**, *38*, 3098.
(28) Wilk, L.; Vosko, S. H.; Nusair, M. *Can. J. Phys.* **1980**, *58*, 1200.
(29) Lee, C.; Yang, W.; Parr, R. G. *Phys. Rev. B* **1988**, *37*, 785.
(30) Perdew, J. P. *Phys. Rev. B* **1986**, *33*, 8822.
(31) Hariharan, P. C.; Pople, J. A. *Theor. Chim. Acta* **1973**, *28*, 213.
(32) Francl, M. M.; Petro, W. J.; Hehre, W. J.; Binkley, J. S.; Gordon, M. S.; DeFrees, D. J.; Pople, J. A. *J. Chem. Phys.* **1982**, *77*, 3654.
(33) Perdew, J. P.; Wang, Y. *Phys. Rev. B* **1986**, *33*, 8800.
(34) Perdew, J. P. *Phys. Rev. B* **1986**, *33*, 8822.
(35) Perdew, J. P. *Phys. Rev.* **1986**, *34*, 7406.
(36) Kutzelnigg, W.; Fleischer, U.; Schindler, M. *NMR - Basic Principles and Progress*; Springer-Verlag: Heidelberg, 1990; Vol. 23.
(37) St-Amant, A.; Salahub, D. R. *Chem. Phys. Lett.* **1990**, *169*. 387.
(38) St-Amant, A. Ph.D. Thesis, Université de Montréal, 1991.
(39) Salahub, D. R.; Fournier, R.; Mlynarski, P.; Papai, I.; St-Amant, A.; Ushio, J. *Density Functional Methods in Chemistry*; Labanowski, J., Andzelm, J., Eds.; Springer: New York, 1991.
(40) Daul, C.; Goursot, A.; Salahub, D. R. *Grid Methods in Atomic and Molecular Quantum Calculations*; Cerjan, C., Ed.; NATO Advanced Study Institute C142; 1993; Vol. 23.
(41) Krishnan, R.; Pople, J. A. *Int. J. Quant. Chem.* **1978**, *14*, 91.
(42) Krishnan, R.; Binkley, J. S.; Seeger, R.; Pople, J. A. *J. Chem. Phys.* **1980**, *72*, 650.
(43) McLean, A. D.; Chandler, G. S. J. Chem. Phys. 1980, 72, 5639.
(44) Clark, T.; Chandrasekhar, J.; Spitznagel, G. W.; von R. Schleyer, P. *J. Comput. Chem.* **1983**, *4*, 294.
(45) Gill, P. M. W.; Johnson, B. G.; Pople, J. A.; Frisch, M. *J. Chem. Phys. Lett.* **1992**, *197*, 499.
(46) Frisch, M. J.; Pople, J. A.; Binkley, J. S.; von R. Schleyer, P. *J. Chem. Phys.* **1984**, *80*, 3265.
(47) Fermi, E. *Z. Phys.* **1930**, *60*, 320.
(48) Fermi, E.; Segré, E. *Z. Phys.* **1933**, *82*, 729.
(49) Gonzalez, C.; Schlegel, H. B. *J. Chem. Phys.* **1989**, *90*, 2154.
(50) Gonzalez, C.; Schlegel, H. B. *J. Phys. Chem.* **1990**, *94*, 5523.
(51) Boys, S. F.; Bernardi, F. *Mol. Phys.* **1970**, *19*, 553.
(52) Scott, A. P.; Radom, L. *J. Phys. Chem.* **1996**, *100*, 16502.